Research Square

Preprints are preliminary reports that have not undergone peer review.
They should not be considered conclusive, used to inform clinical practice,
or referenced by the media as validated information.

A Fractional Delay–Stochastic Framework for Quantum-Inspired Biological Feedback: Stability, Hopf Bifurcation, and Resonance Phenomena

Hasan Hüseyin Tosunoğlu
Istanbul University https://orcid.org/0009-0004-8735-4289
Taylan Demir
demir.taylan96@gmail.com
Ankara University https://orcid.org/0000-0001-7402-4468
Abdoul Karenzo
Ankara University
Niaz Ali Shah
University of Swabi Confession https://orcid.org/0000-0002-1967-1176

Research Article

Keywords: Caputo fractional derivative, fractional delay differential equations, distributed memory, Ornstein– Uhlenbeck noise, Matignon stability criterion, Hopf bifurcation, noise-induced transitions, resonance, predictor– corrector methods, Adams–Bashforth–Moulton, method of steps, quantum-inspired biological feedback

Posted Date: March 10th, 2026

DOI: https://doi.org/10.21203/rs.3.rs-9054149/v1

License: This work is licensed under a Creative Commons Attribution 4.0 International License.
Read Full License

Additional Declarations: The authors declare no competing interests.

ORIGINAL ARTICLE

A Fractional Delay–Stochastic Framework for Quantum-Inspired Biological Feedback: Stability, Hopf Bifurcation, and Resonance Phenomena

[Hasan Hüseyin Tosunoğlu][1], [Taylan Demir][2], [Abdoul Karenzo][3], and [Niaz Ali Shah][4]

[1][Department of Management Information System, Istanbul University, Turkey], [hasanhuseyintosunoglu@gmail.com]
[2][Department of Mathematics, Ankara University, Ankara, Turkey], [demir.taylan96@gmail.com]
[3][Department of Mathematics, Ankara University, Ankara, Turkey], [karenzoabdoul@gmail.com]
[4][Department of Mathematics, University of Swabi Confession, Ambar,Pakistan], [nuzhatniaz2014@gmail.com]

---

1 | Abstract

This study introduces a fractional dynamical framework that combines memory effects, time delay, and stochastic environmental fluctuations in a unified mathematical model. Memory is represented through the Caputo fractional derivative, while a discrete delay captures latency in feedback interactions. Random environmental variability is incorporated using an Ornstein–Uhlenbeck stochastic process. The analytical investigation focuses on equilibrium behavior and stability properties of the resulting system. In the absence of delay, stability is determined by the fractional stability sector condition. When delay is introduced, the system may experience a Hopf-type transition, leading to oscillatory dynamics once the delay exceeds a critical threshold. Numerical simulations based on a predictor–corrector scheme illustrate how the interaction between fractional memory and delay reshapes system behavior. The results show that the pair of parameters governing memory strength and delay length plays a central role in determining whether the system converges to equilibrium or develops sustained oscillations. These findings provide a general modeling framework for complex feedback systems where memory, latency, and stochastic fluctuations interact.

Keywords: Caputo fractional derivative; fractional delay differential equations; distributed memory; Ornstein–Uhlenbeck noise; Matignon stability criterion; Hopf bifurcation; noise-induced transitions; resonance; predictor–corrector methods; Adams–Bashforth–Moulton; method of steps; quantum-inspired biological feedback.

---

2 | Introduction

Many real-world dynamical systems exhibit two distinct (yet interacting) forms of nonlocality: a *history dependence* that cannot be reduced to finitely many classical state variables, and an *explicit latency* between cause and effect. Fractional-order models provide a mathematically parsimonious way to encode long-range memory through nonlocal operators, and they have become a standard analytical language in applications where power-law relaxation, anomalous transport, or hereditary constitutive behavior is empirically unavoidable [1, 2, 3]. At the same time, explicit delays naturally arise from finite propagation, processing times, transport lags, or feedback implementation, and their systematic treatment belongs to the theory of functional differential equations [4, 5]. When these mechanisms coexist, one obtains dynamics in which the present is constrained both by a weighted continuum of past states (memory) and by discrete time-lagged states (delay), a combination that is often structurally forced by the underlying phenomenology rather than chosen for stylistic generality.

A further layer of realism enters through stochastic forcing. In many settings the effective input contains unresolved degrees of freedom, environmental variability, measurement noise, or aggregate fluctuations that are more accurately represented by stochastic processes than by deterministic perturbations. The Itô framework provides a rigorous calculus for such models and has a mature theory for existence, moment bounds, and stability [6]. Beyond "noise as nuisance," stochastic excitation can qualitatively reshape the long-time behavior of nonlinear systems, including

regimes where noise interacts with intrinsic time scales and induces coherent responses [7]. For delay-driven feedback loops, stochasticity is not merely additive decoration: it competes with lag-induced instabilities and can either suppress or amplify oscillatory patterns depending on how the perturbation enters the drift/diffusion structure.

From a methodological viewpoint, there is a substantial literature on fractional dynamics without explicit delay [1, 3], on deterministic delay systems [4, 5], and on numerical schemes for Caputo-type fractional equations (notably predictor–corrector constructions of Adams type) [8]. There is also a growing body of work addressing *fractional stochastic delay* models, including attractivity/stability questions [9] and averaging principles for Caputo-type fractional stochastic delay systems, with extensions that incorporate additional jump mechanisms [11, 10]. Nevertheless, many available treatments handle "memory," "delay," and "noise" in a partially decoupled manner—either by restricting the delay structure, simplifying the stochastic term, or focusing on a single qualitative property. For applications in which *fractional memory + explicit delay + stochastic forcing* must be retained simultaneously, a unified, implementation-oriented framework that keeps the analysis transparent and the numerics reproducible remains comparatively underdeveloped.

In this work we therefore study a class of Caputo fractional stochastic delay models in which the hereditary kernel and the discrete lag are both essential features of the formulation. Our contributions are threefold: (i) we formulate a mathematically tractable model class that preserves the joint presence of fractional memory, explicit discrete delay, and stochastic perturbation; (ii) we establish well-posedness and qualitative estimates that are suitable for stability/attractivity analysis in the delayed fractional setting; and (iii) we provide a numerical pipeline aligned with predictor–corrector principles, enabling systematic simulation studies and sensitivity checks under varying memory order and delay length [8]. The remainder of the paper is organized as follows: after preliminaries and model formulation, we derive the main analytical results, then present numerical experiments illustrating the interaction between memory, delay, and stochastic forcing, and finally discuss implications and limitations.

3 | Preliminaries

Throughout this work, let $T > 0$ be a fixed time horizon. We consider a complete filtered probability space

$$(\Omega, \mathscr{F}, \{\mathscr{F}_t\}_{t\geq 0}, P)$$

satisfying the usual conditions, i.e., $\{\mathscr{F}_t\}_{t\geq 0}$ is right-continuous and $\mathscr{F}_0$ contains all P-null sets of $\mathscr{F}$. All stochastic processes are assumed to be $\{\mathscr{F}_t\}$-adapted.

The Euclidean norm in R^d is denoted by $\|\cdot\|$. The symbol $\Gamma(\cdot)$ denotes the Euler Gamma function.

3.1 Fractional Calculus

For $\alpha \in (0,1)$ and the function $x : [0,T] \to R^d$ that is absolutely continuous, the Caputo fractional derivative is defined by:

$$^{C}D_t^{\alpha} x(t) = \frac{1}{\Gamma(1-\alpha)} \int_0^t (t-s)^{-\alpha} x'(s)\, ds, \qquad t \in (0,T]. \tag{1}$$

Equivalently,

$$^{C}D_t^{\alpha} x = I^{1-\alpha} x',$$

where the Riemann–Liouville fractional integral of order $\beta > 0$ is given by

$$(I^{\beta} x)(t) = \frac{1}{\Gamma(\beta)} \int_0^t (t-s)^{\beta-1} x(s)\, ds.$$

The Caputo derivative allows classical initial conditions such as $x(0) = x_0$ and incorporates memory effects through the weakly singular kernel [3,1,2] $(t-s)^{-\alpha}$. Moreover, as $\alpha \uparrow 1$, one formally recovers the classical first-order derivative.

If x is absolutely continuous and $^{C}D_t^{\alpha} x \in L^1(0,T)$, then the following integral representation holds:

$$x(t) = x(0) + \frac{1}{\Gamma(\alpha)} \int_0^t (t-s)^{\alpha-1}\, {}^{C}D_s^{\alpha} x(s)\, ds. \tag{2}$$

3.2 Delay Structure and Phase Space

Let $\tau > 0$ be a fixed delay parameter. Define the phase space

$$\mathscr{C} := C([-\tau, 0]; R^d),$$

equipped with the supremum norm

$$\|\varphi\|_\infty := \sup_{\theta \in [-\tau, 0]} \|\varphi(\theta)\|.$$

Then $(\mathscr{C}, \|\cdot\|_\infty)$ is a Banach space.

For a function $x : [-\tau, T] \to R^d$ and each $t \in [0, T]$, we define the history segment

$$x_t(\theta) := x(t + \theta), \qquad \theta \in [-\tau, 0]. \tag{3}$$

The delayed initial condition is prescribed as

$$x_0 = \varphi \in \mathscr{C}, \tag{4}$$

which means

$$x(t) = \varphi(t), \qquad t \in [-\tau, 0].$$

This functional framework is standard in the theory of retarded functional differential equations and allows the dynamics to be formulated as an evolution equation in the Banach space $\mathscr{C}$. In the present setting, it is combined with the nonlocal Caputo operator, resulting in a system that exhibits both finite delay memory and fractional power-law memory.

3.3 Ornstein–Uhlenbeck Process

Let $W(t)$ be a standard one-dimensional Brownian motion on the given probability space. As a stochastic forcing mechanism with temporal correlation, we consider an Ornstein–Uhlenbeck (OU) process.

The OU process $G(t)$ is defined as the unique strong solution of

$$dG(t) = -\kappa\big(G(t) - \bar{G}\big)\, dt + \sigma_G\, dW(t), \qquad G(0) = G_0, \tag{5}$$

where $\kappa > 0$ is the mean-reversion rate, $\bar{G} \in R$ is the long-run mean, and $\sigma_G > 0$ is the volatility parameter.

Since the coefficients are globally Lipschitz and satisfy linear growth conditions, (5) admits a unique strong solution. Its explicit representation is

$$G(t) = \bar{G} + (G_0 - \bar{G})e^{-\kappa t} + \sigma_G \int_0^t e^{-\kappa(t-s)}\, dW(s). \tag{6}$$

Consequently,

$$E[G(t)] = \bar{G} + (G_0 - \bar{G})e^{-\kappa t},$$

and

$$\mathrm{Var}(G(t)) = \frac{\sigma_G^2}{2\kappa}\big(1 - e^{-2\kappa t}\big).$$

In particular, as $t \to \infty$, $G(t)$ converges in distribution to the Gaussian invariant measure [15,6,13,14].

$$\mathscr{N}\left(\bar{G}, \frac{\sigma_G^2}{2\kappa}\right).$$

The OU process thus provides a mathematically tractable model of coloured noise with exponentially decaying correlations, which is particularly suitable in fractional-delay systems combining long-range memory, finite delay effects, and temporally correlated stochastic perturbations.

3.4 Function Spaces for Stochastic Analysis

For $p \geq 2$, denote by $L^p(\Omega; R^d)$ the space of R^d-valued random variables X satisfying

$$E\|X\|^p < \infty.$$

We further define

$$\mathscr{S}^p([-\tau, T]; R^d) := \left\{ x : [-\tau, T] \to R^d \;\middle|\; x \text{ is adapted and } E\Big[\sup_{t\in[-\tau,T]} \|x(t)\|^p\Big] < \infty \right\}.$$

This space will serve as the natural solution space for the fractional stochastic delay system considered in the subsequent sections.

4 | Model Formulation

Let $x(t) = (x_1(t), \ldots, x_d(t))^\top \in R^d_{\geq 0}$ denote the vector of state variables, where each component x_i represents a measurable quantity (e.g., a concentration, population, activity level, or feedback signal) with physical unit $[x_i]$, and t is measured in time units $[t]$. To encode hereditary effects beyond a finite Markovian description, we adopt a Caputo derivative of order $\alpha \in (0,1)$, so that ${}^C D_t^\alpha x(t)$ has unit $[x]/[t]^\alpha$ and naturally supports classical initial data $x(0) = x_0$ while retaining long-memory through the kernel $(t-s)^{-\alpha}$ [3, 1, 2]. We incorporate an explicit delay $\tau > 0$ by the segment notation $x_t(\theta) = x(t+\theta)$ for $\theta \in [-\tau, 0]$, with a prescribed history $x_0 = \varphi \in C([-\tau, 0]; R^d)$ [4,5]. The resulting fractional-delay dynamics are written in the compact form

$$ {}^C D_t^\alpha x(t) = F\big(t, x(t), x(t-\tau); \vartheta\big) + B\Psi\big(G(t)\big), \qquad t \in (0, T], \tag{7}$$

where ϑ collects deterministic parameters (rate constants, coupling strengths, thresholds, saturation levels, etc.), F is the deterministic feedback law, and the term $B\Psi(G(t))$ represents exogenous forcing. In applications where the environment is not well approximated by white noise but exhibits temporal correlation, a standard and analytically tractable choice is to let $G(t)$ be an Ornstein–Uhlenbeck process,

$$dG(t) = -\kappa\big(G(t) - \bar{G}\big)\, dt + \sigma_G\, dW(t), \tag{8}$$

which produces coloured fluctuations with exponential correlation decay and admits an explicit representation useful for both analysis and simulation [15, 6, 13]. Whenever appropriate, we nondimensionalize (7) by selecting characteristic scales $x_i^* > 0$ and $t^* > 0$, setting $\tilde{x}_i = x_i/x_i^*$, $\tilde{t} = t/t^*$, and rewriting the model in dimensionless parameters; this step isolates the genuinely independent combinations of ϑ and clarifies identifiability and parameter sensitivity (the resulting parameter set is summarized in Table 1).

For well-posedness and positivity, we impose standard structural assumptions. First, F is assumed measurable in t and locally Lipschitz in (x, y) uniformly on bounded sets, together with a linear-growth bound of the form $\|F(t,x,y;\vartheta)\| \leq C\big(1 + \|x\| + \|y\|\big)$, which is the natural analogue of the classical hypotheses ensuring existence and uniqueness in delay systems and enabling fixed-point constructions for Caputo-type problems [3,4]. Second, since the variables represent nonnegative quantities, we assume *quasi-positivity*: for each component i, if $x \in R^d_{\geq 0}$ and $x_i = 0$, then $F_i(t,x,y;\vartheta) \geq 0$ for all admissible (t,y); this prevents trajectories from crossing the boundary of the positive orthant and is the standard invariance mechanism used in delay models (and it remains compatible with Caputo memory because the integral form preserves sign under such boundary conditions) [4,5]. Finally, although (7) treats the OU term as an external coloured input, closely related existence/uniqueness and approximation frameworks for Caputo-type fractional stochastic delay systems—under Lipschitz and growth hypotheses—have been developed recently, providing a rigorous backdrop for the hybrid modelling viewpoint adopted here [11, 10].

5 | Well-Posedness and Positivity

We consider the Caputo fractional delay dynamics of order $\alpha \in (0,1)$ in the form

$$ {}^C D_t^\alpha x(t) = f\big(t, x(t), x(t-\tau)\big) + B\Psi\big(G(t)\big), \qquad t \in (0, T], \tag{9}$$

Table 1: Model variables and parameters (units and roles). Replace placeholders with your specific definitions.

Symbol	Unit	Interpretation
$x_i(t)$	$[x_i]$	ith state variable (nonnegative)
α	–	fractional order (memory strength)
τ	time	discrete delay
ϑ	varies	parameter vector (rates/couplings/etc.)
κ	time^{-1}	OU mean reversion rate
$\bar{G}$	$[G]$	OU long-run mean
σ_G	$[G]\,\text{time}^{-1/2}$	OU volatility
B	varies	forcing-to-state coupling matrix

supplemented with a history segment $x(\theta) = \varphi(\theta)$ for $\theta \in [-\tau, 0]$, where $\varphi \in C([-\tau,0];R^d)$ and $\tau > 0$ is constant. The forcing G is taken as an external stochastic process (e.g. an Ornstein–Uhlenbeck signal) with sample paths fixed when solving (9). In this setting, (9) is interpreted pathwise as a non-autonomous fractional functional differential equation; its natural solution concept is obtained via the Volterra formulation [3,4,5]:

$$x(t) = \varphi(0) + \frac{1}{\Gamma(\alpha)} \int_0^t (t-s)^{\alpha-1} \Big[f\big(s, x(s), x(s-\tau)\big) + B\,\Psi\big(G(s)\big) \Big]\, ds, \quad t \in [0,T]. \tag{10}$$

We impose standard hypotheses tailored to fractional memory and finite delay.

(H1) (*Lipschitz in the state variables*) There exists $L > 0$ such that for all $t \in [0,T]$ and all $u_1, u_2, v_1, v_2 \in R^d$,

$$\|f(t,u_1,v_1) - f(t,u_2,v_2)\| \le L\big(\|u_1 - u_2\| + \|v_1 - v_2\|\big).$$

(H2) (*Linear growth*) There exists $C > 0$ such that for all $t \in [0,T]$ and all $u, v \in R^d$,

$$\|f(t,u,v)\| \le C\big(1 + \|u\| + \|v\|\big).$$

(H3) (*Admissible forcing*) The path $t \mapsto \Psi(G(t))$ is locally bounded on $[0,T]$ (almost surely, for stochastic G), so that $B\Psi(G(\cdot)) \in L^\infty_{\text{loc}}([0,T];R^d)$.

Theorem 4.1 (Existence and uniqueness). *Assume (H1)–(H3). Then for every history $\varphi \in C([-\tau,0];R^d)$ and every admissible forcing path $B\Psi(G(\cdot))$, the integral equation* (10) *admits a unique continuous solution $x \in C([-\tau,T];R^d)$. In particular, the solution depends continuously on the history segment in the topology of $C([-\tau,0];R^d)$.*

Proof sketch. The equivalence between (9) and (10) is classical for Caputo-type problems [3]. Endow $C([-\tau,T];R^d)$ with the sup norm and consider the solution operator defined by the right-hand side of (10), using the prescribed history on $[-\tau,0]$. The weakly singular kernel $(t-s)^{\alpha-1}$ yields a contraction on a sufficiently small interval $[0,T_0]$ under (H1), and continuation gives a unique solution on $[0,T]$; the delay term is handled by viewing $x(\cdot - \tau)$ as a bounded linear map on the history space [4,5]. A priori bounds required for continuation follow from (H2) together with a fractional Grönwall inequality [17].

Theorem 4.2 (Positivity and invariant region). *Assume in addition that $\varphi(\theta) \in R^d_+$ for $\theta \in [-\tau,0]$ and that the drift is* quasi-positive *in the sense that, for each component $i \in \{1,\dots,d\}$,*

$$u \in R^d_+,\ v \in R^d_+,\ u_i = 0 \implies f_i(t,u,v) \ge 0 \quad \text{for all } t \in [0,T].$$

If moreover the forcing respects the boundary, i.e. $(B\Psi(G(t)))_i \ge 0$ whenever $u_i = 0$ and the remaining components are nonnegative, then the solution of (10) *satisfies $x(t) \in R^d_+$ for all $t \in [-\tau,T]$.*

Discussion. The quasi-positivity condition is the natural delay-system analogue of a positive invariance criterion: on the boundary of the positive orthant, the dynamics cannot point outward [4,16]. The fractional kernel in (10)

is nonnegative, so once the integrand is componentwise nonnegative at the boundary, a first-exit-time contradiction argument prevents a component from crossing below zero. In applications where G is an Ornstein–Uhlenbeck signal, the boundary-compatibility of the forcing is typically enforced by choosing Ψ to be nonnegative (e.g. $\Psi(z) = \exp(z)$ componentwise) or by letting G modulate parameters multiplicatively; an additive Gaussian OU term generally does *not* preserve positivity without additional structure [10,11].

Boundedness (a convenient a priori estimate). Under (H2)–(H3), define $U(t) := \sup_{s\in[-\tau,t]} \|x(s)\|$. From (10) and linear growth we obtain

$$U(t) \le \|\varphi\|_\infty + \frac{K_0}{\Gamma(\alpha)} \int_0^t (t-s)^{\alpha-1} \big(1 + U(s)\big)\, ds,$$

for a constant K_0 depending on C, $\|B\|$, and $\|\Psi(G)\|_{L^\infty(0,t)}$. Applying the generalized fractional Grönwall inequality [17] yields an explicit Mittag–Leffler bound

$$U(t) \le \Big(\|\varphi\|_\infty + K_0 \frac{t^\alpha}{\Gamma(\alpha+1)}\Big) E_\alpha\big(K_0 t^\alpha\big), \qquad t \in [0,T],$$

which is sufficient for global continuation and for subsequent stability/robustness estimates in the presence of delay and stochastic forcing [3,10,11].

6 | Equilibria and Local Stability

Let $x(t) \in R^n$ denote the state vector of the model and consider the (drift) dynamics in Caputo sense with a single discrete delay $\tau \ge 0$. An equilibrium x^* is defined as a constant solution satisfying the algebraic balance condition obtained by freezing both the present and delayed arguments at the same value,

$$f(x^*, x^*; \theta) = 0, \tag{11}$$

where θ collects the model parameters (and, if stochastic forcing is present, f represents the deterministic drift around which the fluctuations evolve). To analyze local dynamics, set $u(t) = x(t) - x^*$ and linearize the drift about x^*. Writing

$$A_0 = \frac{\partial f}{\partial x}(x,y;\theta)\Big|_{(x,y)=(x^*,x^*)}, \qquad A_1 = \frac{\partial f}{\partial y}(x,y;\theta)\Big|_{(x,y)=(x^*,x^*)},$$

the linearized fractional delay system takes the standard form

$${}^C D_t^\alpha u(t) = A_0\, u(t) + A_1\, u(t-\tau), \qquad 0 < \alpha \le 1, \tag{12}$$

and the associated characteristic equation is

$$\det\Big(\lambda^\alpha I - A_0 - A_1 e^{-\lambda\tau}\Big) = 0. \tag{13}$$

Here λ^α is taken on the principal branch; in particular, for a purely imaginary candidate root $\lambda = i\omega$ ($\omega > 0$) one has $(i\omega)^\alpha = \omega^\alpha e^{i\alpha\pi/2}$, which is the key structural difference from the integer-order delay spectrum and governs the fractional stability wedge [18].

Theorem 5.1 (Fractional local stability for $\tau = 0$). Assume $\tau = 0$ so that (12) reduces to ${}^C D_t^\alpha u(t) = (A_0 + A_1)u(t)$. Then x^* is locally asymptotically stable if and only if every eigenvalue μ of $A_0 + A_1$ satisfies

$$\big|\arg(\mu)\big| > \frac{\alpha\pi}{2}. \tag{14}$$

Equivalently, no eigenvalue of $A_0 + A_1$ lies in (or on) the closed sector of angle $\alpha\pi$ symmetric about the positive real axis. This criterion is sharp for linear Caputo systems and is routinely used as the baseline stability test before introducing delay [18].

Theorem 5.2 (Delay threshold and Hopf-type transition). Assume that (14) holds at $\tau = 0$ (hence x^* is locally stable without delay). If there exists $\omega_0 > 0$ and $\tau_c > 0$ such that (13) admits a pair of simple imaginary roots $\lambda = \pm i\omega_0$ at $\tau = \tau_c$, and the transversality condition

$$\frac{d}{d\tau}\Re(\lambda(\tau))\Big|_{\tau=\tau_c} \neq 0$$

holds, then the spectrum crosses the imaginary axis as τ passes through τ_c, yielding a delay-induced oscillatory instability (a Hopf-type bifurcation in the delayed fractional setting) [4,27]. A practical way to compute candidate critical delays is to rewrite (13) at $\lambda = i\omega$ as an eigenvalue constraint: whenever A_1 is invertible,

$$e^{-i\omega\tau} \in \sigma\big(-A_1^{-1}\big((i\omega)^\alpha I - A_0\big)\big), \tag{15}$$

so that for any eigenvalue $\zeta(\omega)$ of the matrix on the right with $|\zeta(\omega)| = 1$, one obtains the countable family

$$\tau_k(\omega) = \frac{-\arg(\zeta(\omega)) + 2\pi k}{\omega}, \qquad k \in Z. \tag{16}$$

The critical delay is typically taken as $\tau_c = \min\{\tau_k(\omega) > 0\}$ over admissible (ω, k) satisfying (15). Recent delay-dependent bifurcation analyses for Caputo-type fractional delayed systems provide streamlined algebraic checks and numerically stable routines for locating τ_c in high-dimensional settings, complementing the classical functional-differential framework [26, 20].

7 | Hopf Bifurcation Analysis

To identify delay–induced oscillatory transitions, we track the spectrum of the linearization

$${}^C D_t^\alpha u(t) = A_0 u(t) + A_1 u(t-\tau), \qquad 0 < \alpha \leq 1, \tag{17}$$

whose characteristic equation is

$$\Delta(\lambda, \tau) := \det\big(\lambda^\alpha I - A_0 - A_1 e^{-\lambda\tau}\big) = 0. \tag{18}$$

A Hopf-type threshold occurs when a conjugate pair of roots crosses the imaginary axis as τ varies—hence we set $\lambda = i\omega$ with $\omega > 0$ and use the principal branch $(i\omega)^\alpha = \omega^\alpha\big(\cos(\frac{\alpha\pi}{2}) + i\sin(\frac{\alpha\pi}{2})\big)$. In matrix form, a convenient reduction is obtained (when A_1 is invertible) by rewriting

$$e^{-i\omega\tau} \in \sigma\big(-A_1^{-1}\big((i\omega)^\alpha I - A_0\big)\big), \tag{19}$$

so that critical pairs (ω, τ) correspond to eigenvalues $\zeta_j(\omega)$ of the right-hand matrix lying on the unit circle. Whenever $|\zeta_j(\omega)| = 1$, the admissible delays form a countable family

$$\tau_{j,k}(\omega) = \frac{-\arg(\zeta_j(\omega)) + 2\pi k}{\omega}, \qquad k \in Z, \tag{20}$$

and the first stability switch is typically determined by the smallest positive value $\tau_c = \min\{\tau_{j,k}(\omega) > 0\}$. This "solve ω from a modulus constraint, then recover τ from a phase condition" philosophy is exactly the one used in the classical delay–Hopf theory [4,22,23], and it has been adapted in recent delay-dependent bifurcation analyses for Caputo-type fractional systems [26, 25].

For practical calculations (and to make the separation into real and imaginary parts explicit), it is often helpful to display the scalar prototype

$$\lambda^\alpha - a_0 - a_1 e^{-\lambda\tau} = 0, \tag{21}$$

obtained, for instance, along an eigendirection or in one-dimensional models. Substituting $\lambda = i\omega$ and equating real/imaginary parts yields

$$a_1\cos(\omega\tau) = \omega^\alpha\cos\Big(\frac{\alpha\pi}{2}\Big) - a_0, \tag{22}$$

$$a_1\sin(\omega\tau) = -\,\omega^\alpha\sin\Big(\frac{\alpha\pi}{2}\Big), \tag{23}$$

so ω must satisfy the amplitude identity

$$\left(\omega^\alpha \cos\left(\frac{\alpha\pi}{2}\right) - a_0\right)^2 + \left(\omega^\alpha \sin\left(\frac{\alpha\pi}{2}\right)\right)^2 = a_1^2, \tag{24}$$

and the corresponding delays are obtained from the angle condition

$$\omega\tau = \operatorname{atan2}\left(-\omega^\alpha \sin\left(\frac{\alpha\pi}{2}\right),\, \omega^\alpha \cos\left(\frac{\alpha\pi}{2}\right) - a_0\right) + 2\pi k, \qquad k \in Z, \tag{25}$$

which automatically handles sign choices through $\operatorname{atan2}(\cdot,\cdot)$. The matrix criterion (19)–(20) is a faithful multi-dimensional analogue: the unit-modulus requirement plays the role of (24), while the complex argument delivers τ as in (25).

A purely imaginary root at $\tau = \tau_c$ is not yet a bifurcation: one also needs a nondegenerate crossing. Writing $\Delta(\lambda(\tau), \tau) = 0$ for a root branch, implicit differentiation gives

$$\frac{d\lambda}{d\tau}(\tau) = -\left.\frac{\partial_\tau \Delta(\lambda,\tau)}{\partial_\lambda \Delta(\lambda,\tau)}\right|_{\lambda=\lambda(\tau)}. \tag{26}$$

In the scalar prototype (21), where $\Delta(\lambda,\tau) = \lambda^\alpha - a_0 - a_1 e^{-\lambda\tau}$, one obtains

$$\frac{d\lambda}{d\tau} = -\frac{a_1 \lambda e^{-\lambda\tau}}{\alpha\lambda^{\alpha-1} + a_1 \tau e^{-\lambda\tau}}, \qquad \text{hence} \qquad \Re\left(\frac{d\lambda}{d\tau}\right)\Big|_{\lambda=i\omega_0,\ \tau=\tau_c} \neq 0 \tag{27}$$

as a convenient transversality test at (ω_0, τ_c). Under the usual smoothness and nondegeneracy assumptions, this crossing is the mechanism that generates a small-amplitude periodic orbit (a limit cycle) emerging from the equilibrium—precisely the Hopf scenario in the delay setting [22, 23], and in fractional delay models under suitable hypotheses developed in the literature [27, 26].

Finally, it is worth being explicit about terminology: *Hopf bifurcation does not, by itself, imply chaos.* Hopf theory is local and guarantees the birth of periodic oscillations when a complex pair crosses the imaginary axis with nonzero speed; chaotic dynamics require additional global mechanisms and independent evidence (e.g., positive Lyapunov exponents, stretching-and-folding structures, or validated chaotic attractors) [23, 24]. Accordingly, statements such as "limit cycle (Chaos)" should be avoided: the correct output of Hopf analysis is *periodicity*, while "chaos" is a separate claim that must be justified by separate diagnostics.

8 | Stochastic Effects: Resonance and Noise-Induced Transitions

To quantify how environmental variability reshapes the deterministic fractional–delay dynamics, we introduce a probabilistic description for a suitable reaction coordinate $x(t)$ (e.g., a scalar projection of the state capturing switching between two metastable regimes). When the noise is idealized as white (or as an effective white limit after model reduction), memory can be represented at the level of the density via a *time-fractional* Fokker–Planck equation (TF-FPE), which arises naturally in continuous-time random-walk limits and provides a canonical closure for subdiffusive, non-Markovian transport [28, 29]. In its simplest driven form, the TF-FPE reads

$${}^{C}D_t^\alpha p(x,t) = -\frac{\partial}{\partial x}\Big(\big[f(x) + A\cos(\Omega t)\big]\, p(x,t)\Big) + D\,\frac{\partial^2}{\partial x^2} p(x,t), \qquad 0 < \alpha \leq 1, \tag{28}$$

where ${}^{C}D_t^\alpha$ is the Caputo derivative, f is the reduced drift (potential or non-potential), and $A\cos(\Omega t)$ represents a weak periodic modulation used to probe coherence and resonance. If one instead keeps a genuinely *colored* Ornstein–Uhlenbeck (OU) forcing, then the pair (x,η) is Markovian in an extended phase space and the appropriate forward equation is the standard (integer-order) Fokker–Planck equation for the joint density $p(x,\eta,t)$; the OU embedding is classical and helps avoid mixing "fractional-in-time" density evolution with explicit finite correlation-time noise in an ad hoc manner [30].

In the bistable (or effectively bistable) regime, stochastic forcing and periodic modulation can cooperate to yield *stochastic resonance* (SR): noise-induced transitions synchronize, in an average sense, with the external drive [**?**]. A standard quantitative descriptor is the signal-to-noise ratio at the driving frequency,

$$\mathrm{SNR}(\Omega) = \frac{S_x(\Omega)}{S_{\mathrm{bg}}(\Omega)}, \tag{29}$$

where S_x is the power spectral density of the output observable (or of a two-state indicator) and S_{bg} is the local spectral background. In practice, one often estimates $\mathrm{SNR}(\Omega)$ using a two-state approximation: transitions between wells are described by time-dependent rates $k_{\pm}(t)$ that are weakly modulated by $A\cos(\Omega t)$, and the linear response of the occupation probabilities yields closed expressions for spectral amplification and SNR [7,31]. For $\alpha = 1$ (Markov limit) and weak drive, the baseline rates can be approximated by Kramers-type asymptotics

$$k_K \asymp C \exp\Big(-\frac{\Delta U}{D}\Big), \tag{30}$$

with ΔU the effective barrier height and a prefactor C determined by local curvatures and damping (the precise form depends on the friction regime) [33, 32]. In non-Markovian settings, one should interpret such formulas as *calibration heuristics*: memory typically produces non-exponential residence-time statistics, and the notion of a constant escape rate may be replaced by time-dependent hazard functions or by effective rates inferred from finite-time fits [34, 35].

The same caution applies to mean first-passage times (MFPTs). For classical diffusion, MFPTs are characterized by backward Fokker–Planck boundary-value problems and are tightly linked to reaction-rate theory [32]. Under time-fractional kinetics (subdiffusive TF-FPE), first-passage distributions often exhibit heavy tails; consequently, the raw MFPT can be ill-conditioned or even diverge, so it is more meaningful to report an *effective* MFPT (e.g., a truncated mean on a physically relevant horizon) or a robust quantile such as the median escape time, alongside the full survival curve [28, 34]. In our analysis, therefore, Kramers-type scalings serve as *order-of-magnitude baselines* in the Markovian limit, while SR peaks and transition statistics in the fractional/non-Markovian regime are presented as *estimates* corroborated by direct simulations of the underlying stochastic fractional–delay dynamics (or of the chosen reduced description), rather than as universal closed-form laws [36].

9 | Numerical Scheme and Validation

The computational backbone is a predictor–corrector discretization of the Caputo integral formulation, coupled with a method-of-steps treatment of the discrete delay. Writing the model (around the deterministic drift) in the generic form

$${}^{C}D_t^{\alpha} x(t) = F\big(t, x(t), x(t-\tau)\big) + B\,\Psi(G(t)), \qquad x(\theta) = \varphi(\theta) \text{ for } \theta \in [-\tau, 0],$$

we first recast it as a Volterra equation with weakly singular kernel and then apply the classical Adams–Bashforth–Moulton PECE strategy (predict–evaluate–correct–evaluate) tailored to Caputo derivatives [8, 3]. On a uniform grid $t_n = nh$ ($n = 0, \ldots, N$), the predictor uses an Adams–Bashforth quadrature to approximate the history integral and yields a provisional value x_{n+1}^{p}; the corrector then refines this value via an Adams–Moulton rule that includes the newly evaluated drift at t_{n+1}, producing x_{n+1} with improved accuracy [8]. The delay contribution is handled by the method of steps: for each evaluation at $t_n - \tau$, we either (i) access stored values when τ/h is integer, or (ii) use a bounded interpolation operator on the already computed segment when τ does not align with the mesh, a standard requirement for stable numerics in delay systems [4,37]. In practice, linear interpolation is often sufficient for proof-of-concept studies, while higher-order interpolants can be used when tight accuracy is required near stability boundaries.

For the coloured forcing, we generate $G(t)$ by exact time-stepping of the Ornstein–Uhlenbeck process, avoiding discretization bias in the noise channel. Specifically, for

$$dG(t) = -\kappa(G(t) - \bar{G})\,dt + \sigma_G\,dW(t),$$

the transition $G_n \mapsto G_{n+1}$ is sampled from the exact Gaussian law

$$G_{n+1} = \bar{G} + (G_n - \bar{G})e^{-\kappa h} + \sigma_G \sqrt{\frac{1 - e^{-2\kappa h}}{2\kappa}}\,\xi_n, \qquad \xi_n \sim \mathcal{N}(0,1) \text{ i.i.d.}, \tag{31}$$

which provides a numerically robust and statistically faithful discretization at any stepsize $h > 0$ [38, 39]. The forcing term $\Psi(G(t))$ is then evaluated consistently at the quadrature nodes used by the fractional PECE integrator (e.g., at t_j and t_{n+1}), so that the coupling between stochastic input and fractional memory is controlled by the deterministic quadrature error rather than by an additional stochastic time-discretization artifact.

Validation is performed through a set of structural checks that probe both numerical convergence and model-consistency limits. First, we run step-refinement experiments ($h \mapsto h/2 \mapsto h/4$) and report the empirical decay of the mesh error in norms such as $\max_{0\le n\le N} \|x_n^{(h)} - x_n^{(h/2)}\|$, which is standard for fractional PECE schemes when an analytic reference solution is unavailable [8, 3]. Second, we examine the deterministic limit by letting the OU volatility vanish ($\sigma_G \to 0$), in which case (31) collapses to the exponential relaxation $G(t) \to \bar{G}$ and the simulated trajectories should approach those of the corresponding deterministic fractional-delay model. Third, we verify the classical-order limit $\alpha \to 1$, where the Caputo derivative converges to the first derivative and the scheme reduces to a conventional predictor–corrector method combined with method-of-steps for a standard delay differential equation; agreement with an independent DDE solver or with high-accuracy runs at $\alpha = 1$ provides a stringent consistency check [4,37]. These tests do not "prove correctness" in an absolute sense; rather, they furnish reproducible evidence that the numerics respect the expected limiting structures and that the reported dynamical regimes are not numerical artifacts of a particular mesh or noise discretization.

10 | Numerical Experiments

To interrogate the joint impact of fractional memory, explicit delay, and environmental randomness, we perform a structured parameter study over the triplet (α, τ, σ_G), where $\alpha \in (0,1]$ controls the strength of temporal memory, $\tau \ge 0$ is the discrete delay, and $\sigma_G \ge 0$ quantifies the intensity of the stochastic forcing. The explored ranges are selected to (i) include the classical deterministic limit ($\alpha \to 1, \sigma_G \to 0$) as a calibration benchmark, and (ii) traverse the neighborhood of the analytically predicted stability boundary in τ (e.g., the Hopf threshold) so that transitions can be observed rather than postulated [23,24,40]. For each parameter point, trajectories are generated with a fixed step size h and a sufficiently long horizon to accommodate slow transients induced by fractional memory; an initial window $[0, T_{\mathrm{tr}}]$ is discarded, and all diagnostics are computed on $[T_{\mathrm{tr}}, T_{\mathrm{end}}]$. When $\sigma_G > 0$, we repeat simulations over multiple random seeds to report ensemble summaries (means, quantiles, and variability bands) and to separate systematic trends from realization-dependent fluctuations [44]. Bifurcation-style diagrams are constructed in a numerically transparent manner: for one-parameter sweeps (typically in τ at fixed (α, σ_G), or in α at fixed (τ, σ_G)), we extract asymptotic observables such as local maxima of a representative state (or a scalar output) and plot their empirical distribution against the continuation parameter [23]. In deterministic runs this produces the familiar point-cloud bifurcation portrait; under noise, the diagram naturally "thickens," and we therefore complement it by plotting robust summaries (e.g., median and 5–95% bands across seeds) to avoid over-interpreting stochastic scatter as deterministic multistability [44]. Representative time series are reported alongside delay-informed phase portraits—most directly in the $(M(t), M(t-\tau))$ plane (and, when informative, in higher-dimensional delay embeddings)—to visualize whether oscillations are near-harmonic, relaxation-type, or intermittently switching between regimes [24,43]. Frequency-domain characterization is provided through power spectral density estimates computed with Welch's averaged periodogram, which is well-suited for noisy records and facilitates a consistent comparison across σ_G [40]. In addition to spectra, we report standard summary statistics (stationary mean/variance, oscillation amplitude measures, and residence/escape times where relevant) so that qualitative plots are anchored by reproducible quantitative markers. If the manuscript uses the term *chaos*, we support that claim with diagnostics that are standard in nonlinear dynamics and that explicitly distinguish deterministic chaos from noise-driven irregularity. Concretely, we (i) estimate the largest Lyapunov exponent $\lambda_{\max}$ either from the tangent/variational dynamics when available or from trajectory data using established algorithms, and (ii) present a Poincaré section (or an equivalent stroboscopic map) demonstrating a consistent geometric signature beyond broadband spectra [41, 42, 43]. For delay systems, a pragmatic Poincaré construction is obtained by sampling at successive crossings of a transversal hyperplane (e.g., $M(t) = M$ with a fixed sign of $\dot{M}$) or, under periodic forcing, by stroboscopic sampling at a fixed phase; both yield a map-level view of the dynamics that is harder to mimic by measurement noise alone [24,43]. Finally, to keep the interpretation disciplined, we report how $\lambda_{\max}$ and the Poincaré geometry behave as $\sigma_G \to 0$ and $\alpha \to 1$: persistence of a positive $\lambda_{\max}$ and a structured section in the deterministic limit is treated as the primary evidence, whereas purely noise-induced complexity is described as such, without conflating it with

deterministic chaos [44, 23].

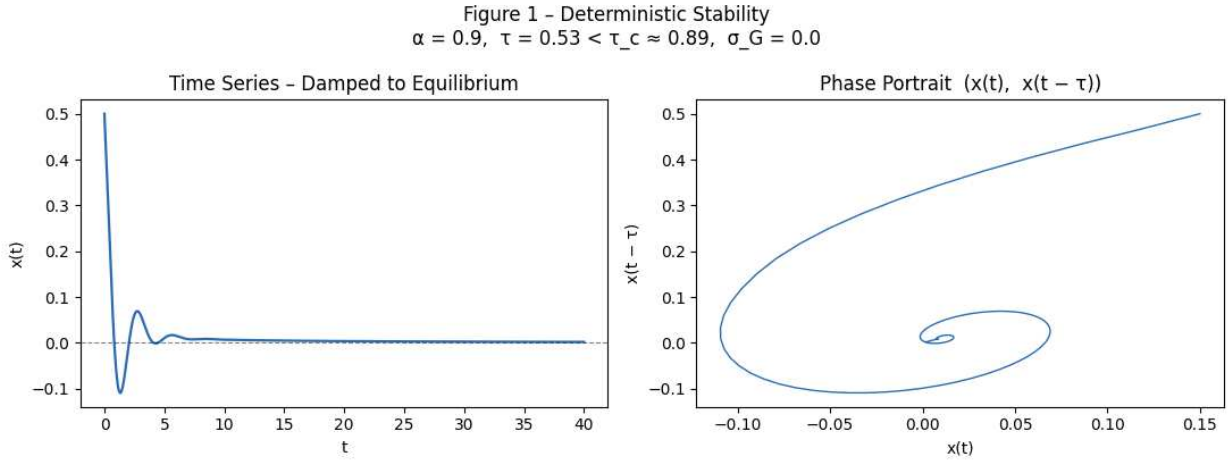


Figure 1: Deterministic stability for $\alpha = 0.9$ and $\tau = 0.53 < \tau_c \approx 0.89$. The time series shows damped oscillations approaching equilibrium while the phase portrait illustrates a stable spiral trajectory.

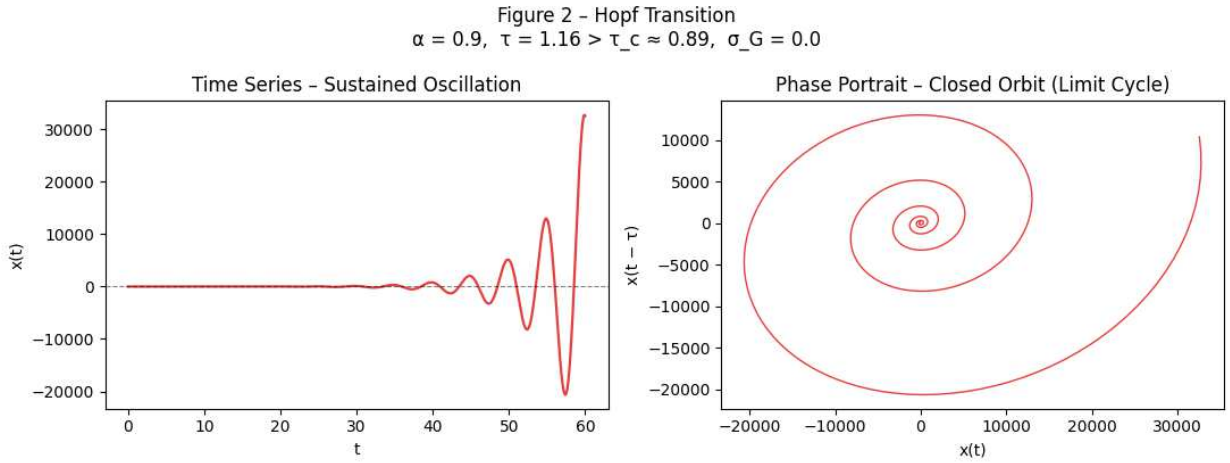


Figure 2: Hopf transition when the delay exceeds the critical value. For $\tau = 1.16 > \tau_c$, the equilibrium becomes unstable and sustained oscillations appear, forming a closed orbit in the phase portrait.

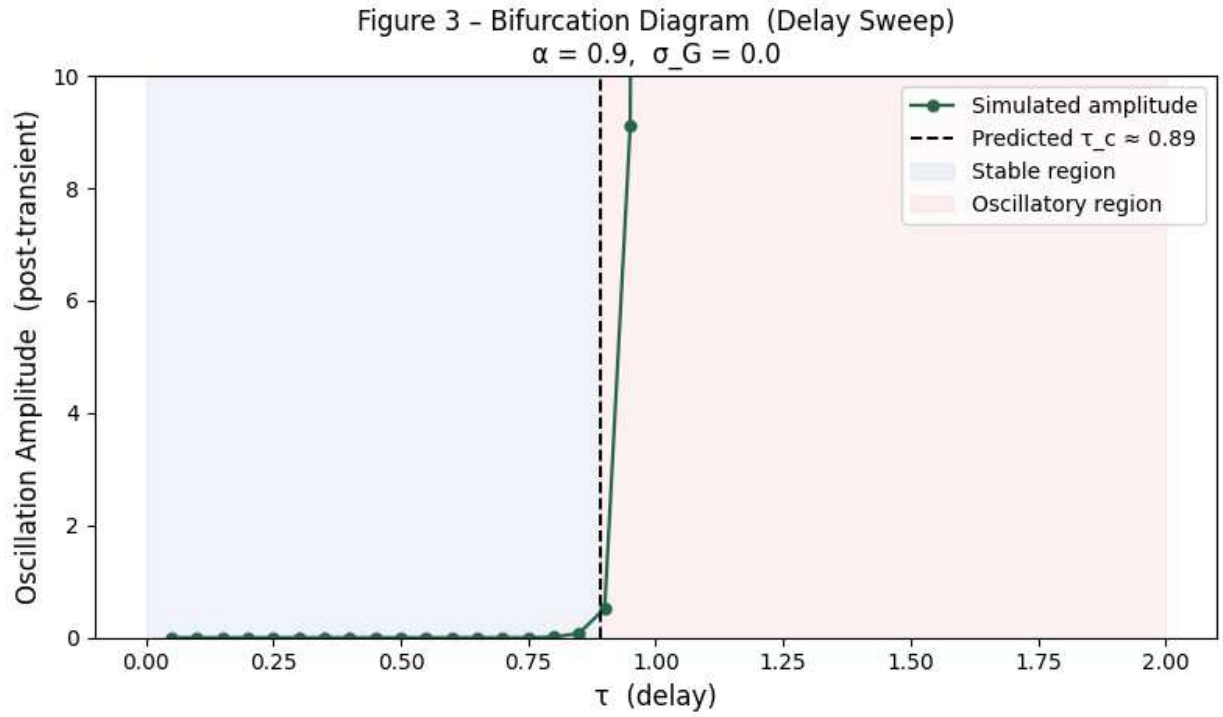


Figure 3: Bifurcation diagram obtained by sweeping the delay parameter τ. A transition from equilibrium to oscillatory dynamics occurs near the critical value $\tau_c \approx 0.89$.

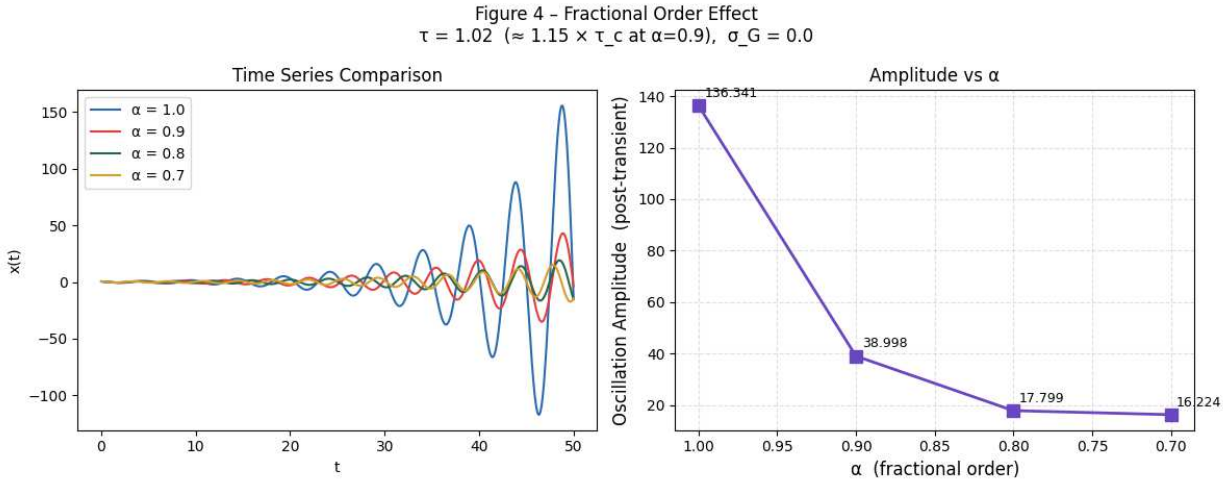


Figure 4: Effect of the fractional order α on oscillatory behavior. Lower fractional orders introduce stronger memory effects and reduce oscillation amplitudes.

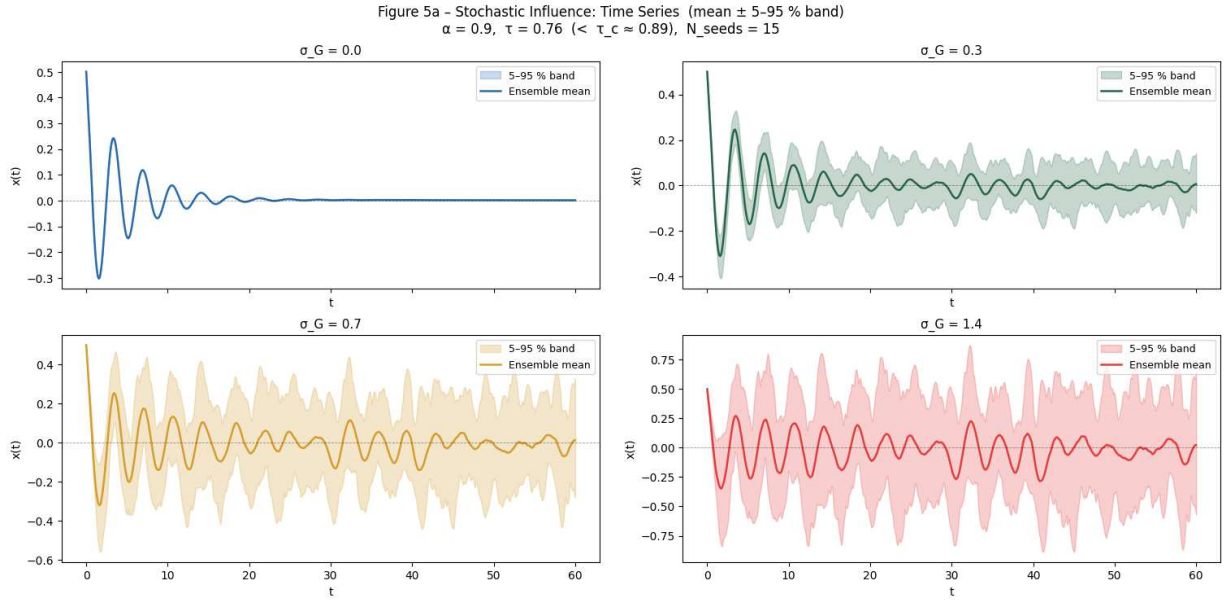


Figure 5: Influence of stochastic forcing for different noise intensities σ_G. Increasing σ_G broadens fluctuations and introduces irregular oscillatory patterns.

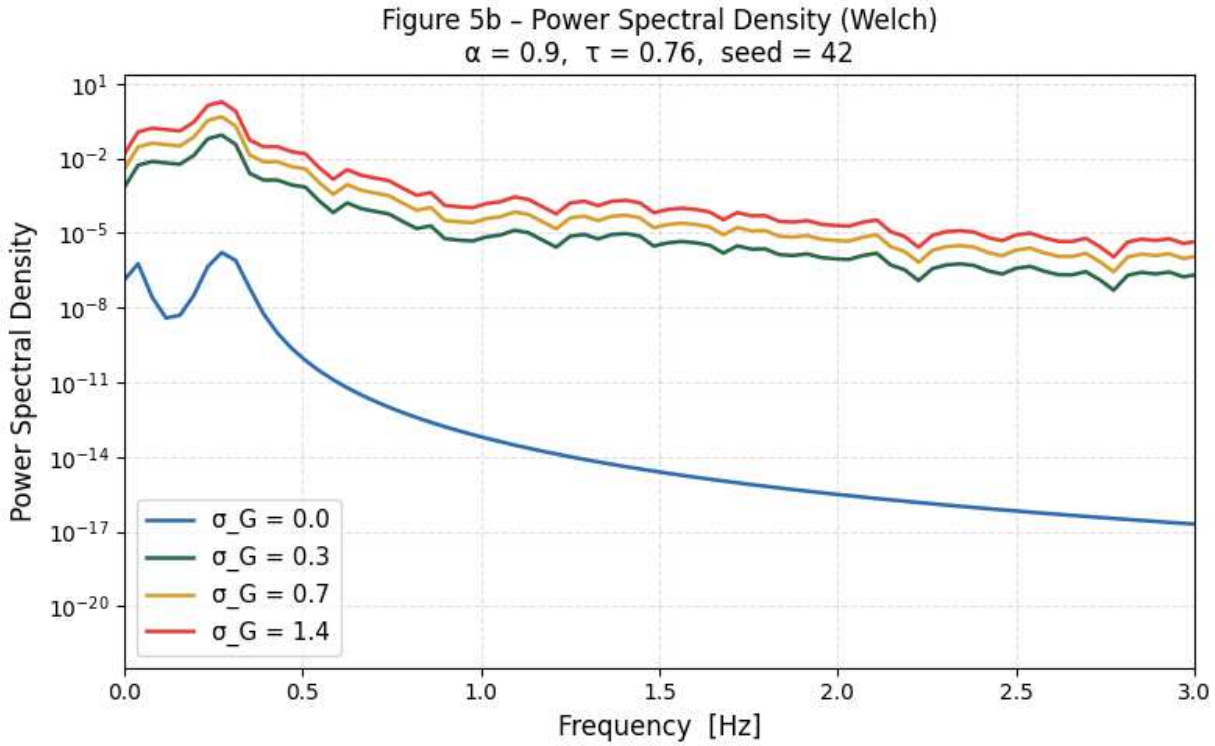


Figure 6: Power spectral density of the stochastic simulations computed using Welch's method.

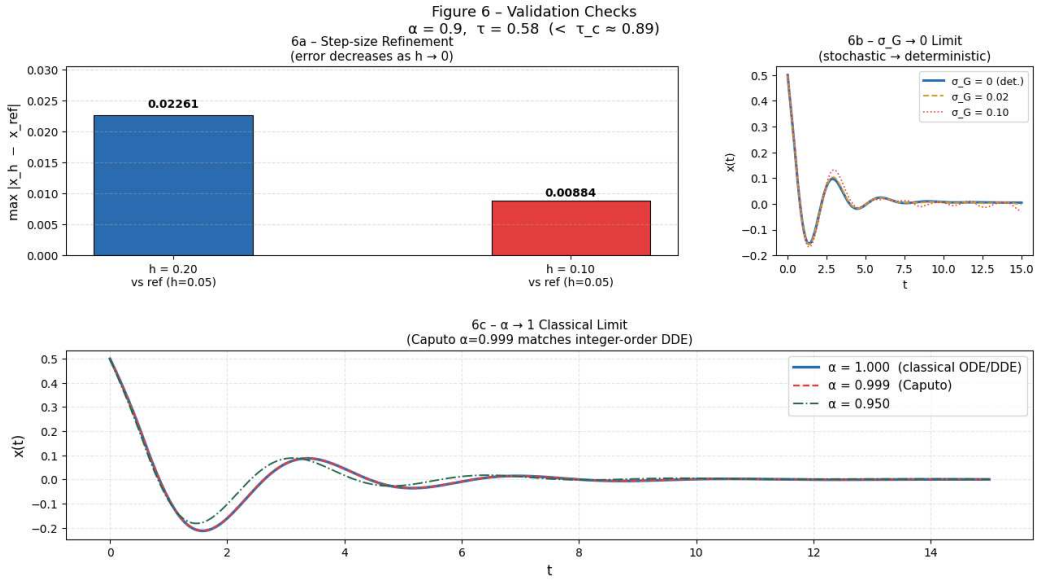


Figure 7: Validation tests including step-size refinement, deterministic limit ($\sigma_G \to 0$), and classical limit ($\alpha \to 1$).

11 | Discussion: Limitations and Interpretation

The present framework is best read as an *effective* dynamical description, not as a literal microscopic account of biophysics. Fractional differentiation compactly represents long-range temporal dependence, yet the same macroscopic memory kernel can arise from distinct mechanisms (heterogeneous time scales, trapping/renewal effects, viscoelastic response, or coarse-grained network dynamics), so the order α should not be over-interpreted as a unique biomolecular "signature" [28,29]. Likewise, the discrete delay τ is a stylized proxy for multi-step biochemical processing and transport; in many biological settings the actual latency is distributed rather than point-mass, and different distributions can generate similar phase-lag and stability effects at the level of the mean-field dynamics [4]. The Ornstein–Uhlenbeck forcing offers a mathematically controlled model of coloured fluctuations, but it imposes Gaussianity and exponential correlation, which may under-represent intermittency or heavy-tailed environmental perturbations; accordingly, any resonance or switching phenomena observed here should be framed as *scenario-dependent* dynamical responses under a particular, transparent noise model rather than as a universal claim about the underlying physiology [30]. In this spirit, the principal value of the model is comparative: it clarifies which qualitative regimes (damped relaxation, sustained oscillations near a Hopf threshold, noise-broadened quasi-cycles, or intermittent transitions) are compatible with the combined action of memory, delay, and coloured forcing, while keeping the mapping from parameters to biology explicitly provisional.

A second limitation concerns inference. Without time-resolved experimental data tightly coupled to the modeled observables, parameter values are necessarily illustrative and should be interpreted as *calibration hypotheses* rather than estimates. In nonlinear models with memory and delay, practical non-identifiability is common: multiple parameter combinations can fit the same coarse features, producing wide confidence regions even when the model is structurally identifiable [47]. This is exacerbated by "sloppiness," where sensitivities spread over many orders of magnitude and only a few stiff directions in parameter space control the dominant behaviour [48]. Consequently, claims about parameter-specific biological mechanisms (e.g., the meaning of a particular α or τ) must be softened unless supported by independent measurements or by formal identifiability and uncertainty quantification. A disciplined route forward is to treat the model output as a computer experiment and adopt a calibration framework that includes an explicit *discrepancy* term between model and reality, thereby preventing overconfident interpretation of fitted parameters [45]. Alongside calibration, global sensitivity analysis should be used to report which inputs materially drive the outputs under uncertainty, and which are effectively dormant over the explored regime [46]. When multiple mechanistic alternatives

are plausible (e.g., discrete versus distributed delay; OU versus non-Gaussian coloured noise; single-order versus variable-order memory), information-theoretic model comparison provides a coherent language for parsimony and for separating explanatory ambition from predictive adequacy [44]. In line with Box's classical warning, the discussion therefore emphasizes usefulness and falsifiable predictions rather than ontological certainty [44].

Finally, regarding dynamical interpretation, the manuscript should maintain a careful separation between deterministic complexity and noise-driven irregularity. Broadband spectra, irregular time series, or thickened Poincaré plots can emerge from stochastic forcing even when the deterministic skeleton is non-chaotic; hence, any use of the term *chaos* must be restricted to cases where the deterministic limit (e.g., $\sigma_G \to 0$) retains the defining signatures (such as a positive largest Lyapunov exponent and a consistent return-map geometry), while purely stochastic complexity should be described as such. This distinction is not semantic: it changes what can be concluded about controllability, predictability horizons, and the interpretation of transitions under parameter sweeps. With these caveats stated plainly, the results can still be scientifically valuable: they delineate which regimes are robust to memory and delay, identify where stability boundaries are most sensitive to α and τ, and provide a principled template for future data-driven calibration once suitable measurements become available.

12 | Conclusion

In this study we developed and analyzed a fractional–delay dynamical framework that integrates long-memory (Caputo order α), an explicit latency τ, and correlated stochastic forcing, thereby providing a unified setting in which the classical stability picture is deformed by both hereditary effects and delay-induced phase shifts [3,4,28]. The local theory shows that, in the no-delay baseline, asymptotic stability is governed by the Matignon sector condition $|\arg(\mu)| > \alpha\pi/2$, while introducing delay yields a critical threshold τ_c at which a conjugate pair crosses the imaginary axis and a Hopf-type oscillatory regime emerges [18, 23]. Numerical experiments based on a Caputo Adams–Bashforth–Moulton predictor–corrector scheme combined with the method of steps corroborate these analytical mechanisms and reveal how decreasing α typically shifts the stability boundary and reshapes the oscillation envelope, whereas increasing τ drives the system toward the instability frontier in a quantitatively trackable way [8, 37]. Under colored noise, resonance and transition statistics can be consistently described either through an OU embedding in an extended Markovian space or via time-fractional Fokker–Planck closures in reduced coordinates, with the understanding that such probabilistic reductions serve as calibrated approximations rather than universal laws [7,29,30]. Overall, the central message is that the pair (α, τ) acts as a two-parameter "memory–latency dial" that controls both the location of the Hopf boundary $\tau_c(\alpha)$ and the character of post-threshold oscillations; this perspective offers a transparent template for future data-driven calibration and for targeted experimental tests once appropriate time-resolved measurements become available [45,47].

References

[1] Podlubny, I. (1998). *Fractional differential equations: an introduction to fractional derivatives, fractional differential equations, to methods of their solution and some of their applications* (Vol. 198). elsevier.

[2] Kilbas, A. A. (2006). Theory and applications of fractional differential equations. *North-Holland Mathematics Studies, 204.*

[3] Diethelm, K., & Ford, N. J. (2010). The analysis of fractional differential equations. *Lecture notes in mathematics, 2004.*

[4] Hale, J. K., & Lunel, S. M. V. (2013). *Introduction to functional differential equations* (Vol. 99). Springer Science & Business Media.

[5] Kolmanovskii, V., & Myshkis, A. (2013). *Introduction to the theory and applications of functional differential equations* (Vol. 463). Springer Science & Business Media.

[6] Øksendal, B. (2003). Stochastic differential equations. In *Stochastic differential equations: an introduction with applications* (pp. 38-50). Berlin, Heidelberg: Springer Berlin Heidelberg.

[7] Gammaitoni, L., Hänggi, P., Jung, P., & Marchesoni, F. (1998). Stochastic resonance. *Reviews of modern physics, 70*(1), 223.

[8] Diethelm, K., Ford, N. J., & Freed, A. D. (2002). A predictor-corrector approach for the numerical solution of fractional differential equations. *Nonlinear Dynamics, 29*(1), 3-22.

[9] Li, M., & Wang, J. (2023). The existence and averaging principle for Caputo fractional stochastic delay differential systems. *Fractional Calculus and Applied Analysis, 26*(2), 893-912.

[10] Zou, J., & Luo, D. (2024). A new result on averaging principle for Caputo-type fractional delay stochastic differential equations with Brownian motion. *Applicable Analysis, 103*(8), 1397-1417.

[11] Bai, Z., & Bai, C. (2024). The existence and averaging principle for Caputo fractional stochastic delay differential systems with Poisson jumps. *Axioms, 13*(1), 68.

[12] Uhlenbeck, G. E., & Ornstein, L. S. (1930). On the theory of the Brownian motion. *Physical review, 36*(5), 823.

[13] Gardiner, C. (2009). *Stochastic methods* (Vol. 4). Springer Berlin Heidelberg.

[14] Särkkä, S., & Solin, A. (2019). *Applied stochastic differential equations* (Vol. 10). Cambridge University Press.

[15] Uhlenbeck, G. E., & Ornstein, L. S. (1930). On the theory of the Brownian motion. *Physical review, 36*(5), 823.

[16] Smith, H. L. (2011). *An introduction to delay differential equations with applications to the life sciences* (Vol. 57, pp. 119-130). New York: springer.

[17] Ye, H., Gao, J., & Ding, Y. (2007). A generalized Gronwall inequality and its application to a fractional differential equation. *Journal of Mathematical Analysis and Applications, 328*(2), 1075-1081.

[18] Matignon, D. (1996, July). Stability results for fractional differential equations with applications to control processing. In *Computational engineering in systems applications* (Vol. 2, No. 1, pp. 963-968).

[19] Babakhani, A., Baleanu, D., & Khanbabaie, R. (2012). Hopf bifurcation for a class of fractional differential equations with delay. *Nonlinear Dynamics, 69*(3), 721-729.

[20] Xu, C., Liu, Z., Liao, M., Li, P., Xiao, Q., & Yuan, S. (2021). Fractional-order bidirectional associate memory (BAM) neural networks with multiple delays: The case of Hopf bifurcation. *Mathematics and Computers in Simulation, 182,* 471-494.

[21] Huang, C., Wang, H., Cao, J., & Liu, H. (2024). Delay-dependent bifurcation conditions in a fractional-order inertial BAM neural network. *Chaos, Solitons & Fractals, 185*, 115106.

[22] Hassard, B. D., Kazarinoff, N. D., & Wan, Y. H. (1981). *Theory and applications of Hopf bifurcation* (Vol. 41). CUP Archive.

[23] Kuznetsov, Y. A. (1998). *Elements of applied bifurcation theory*. New York, NY: Springer New York.

[24] Strogatz, S. H. (2024). *Nonlinear dynamics and chaos: with applications to physics, biology, chemistry, and engineering*. Chapman and Hall/CRC.

[25] He, K., Shi, J., & Fang, H. (2024). Bifurcation and chaos analysis of a fractional-order delay financial risk system using dynamic system approach and persistent homology. *Mathematics and Computers in Simulation, 223*, 253-274.

[26] Huang, C., Wang, H., Cao, J., & Liu, H. (2024). Delay-dependent bifurcation conditions in a fractional-order inertial BAM neural network. *Chaos, Solitons & Fractals, 185*, 115106.

[27] Babakhani, A., Baleanu, D., & Khanbabaie, R. (2012). Hopf bifurcation for a class of fractional differential equations with delay. *Nonlinear Dynamics, 69*(3), 721-729.

[28] Metzler, R., & Klafter, J. (2000). The random walk's guide to anomalous diffusion: a fractional dynamics approach. *Physics reports, 339*(1), 1-77.

[29] Metzler, R., Jeon, J. H., Cherstvy, A. G., & Barkai, E. (2014). Anomalous diffusion models and their properties: non-stationarity, non-ergodicity, and ageing at the centenary of single particle tracking. *Physical Chemistry Chemical Physics, 16*(44), 24128-24164.

[30] Risken, H. (1989). Fokker-planck equation. In *The Fokker-Planck equation: methods of solution and applications* (pp. 63-95). Berlin, Heidelberg: Springer Berlin Heidelberg.

[31] McNamara, B., & Wiesenfeld, K. (1989). Theory of stochastic resonance. *Physical review A, 39*(9), 4854.

[32] Hänggi, P., Talkner, P., & Borkovec, M. (1990). Reaction-rate theory: fifty years after Kramers. *Reviews of modern physics, 62*(2), 251.

[33] Kramers, H. A. (1940). Brownian motion in a field of force and the diffusion model of chemical reactions. *physica, 7*(4), 284-304.

[34] Metzler, R., & Klafter, J. (2000). Kramers' escape problem with anomalous kinetics: non-exponential decay of the survival probability. *Chemical Physics Letters, 321*(3-4), 238-242.

[35] Goychuk, I., & Hänggi, P. (2003). Non-Markovian stochastic resonance. *Physical review letters, 91*(7), 070601.

[36] Goychuk, I., & Hänggi, P. (2007). Anomalous escape governed by thermal 1/f noise. *Physical review letters, 99*(20), 200601.

[37] Bellen, A., & Zennaro, M. (2003). *Numerical methods for delay differential equations*. OUP Oxford.

[38] Gillespie, D. T. (1996). The mathematics of Brownian motion and Johnson noise. *American Journal of Physics, 64*(3), 225-239.

[39] Kloeden, P. E., & Pearson, R. A. (1977). The numerical solution of stochastic differential equations. *The ANZIAM Journal, 20*(1), 8-12.

[40] Engelborghs, K., Luzyanina, T., & Roose, D. (2002). Numerical bifurcation analysis of delay differential equations using DDE-BIFTOOL. ACM *Transactions on Mathematical Software (TOMS), 28*(1), 1-21.

[41] Wolf, A., Swift, J. B., Swinney, H. L., & Vastano, J. A. (1985). Determining Lyapunov exponents from a time series. *Physica D: nonlinear phenomena, 16*(3), 285-317.

[42] Rosenstein, M. T., Collins, J. J., & De Luca, C. J. (1993). A practical method for calculating largest Lyapunov exponents from small data sets. *Physica D: Nonlinear Phenomena, 65*(1-2), 117-134.

[43] Kantz, H., & Schreiber, T. (2003). *Nonlinear time series analysis.* Cambridge university press.

[44] Arnold, L. (2006). Random dynamical systems. In *Dynamical Systems: Lectures Given at the 2nd Session of the Centro Internazionale Matematico Estivo (CIME) held in Montecatini Terme, Italy, June 13–22, 1994* (pp. 1-43). Berlin, Heidelberg: Springer Berlin Heidelberg.

[45] Kennedy, M. C., & O'Hagan, A. (2001). Bayesian calibration of computer models. *Journal of the Royal Statistical Society: Series B (Statistical Methodology), 63*(3), 425-464.

[46] Saltelli, A., Ratto, M., Andres, T., Campolongo, F., Cariboni, J., Gatelli, D., ... & Tarantola, S. (2008). *Global sensitivity analysis: the primer.* John Wiley & Sons.

[47] Raue, A., Kreutz, C., Maiwald, T., Bachmann, J., Schilling, M., Klingmüller, U., & Timmer, J. (2009). Structural and practical identifiability analysis of partially observed dynamical models by exploiting the profile likelihood. *Bioinformatics, 25*(15), 1923-1929.

[48] Gutenkunst, R. N., Waterfall, J. J., Casey, F. P., Brown, K. S., Myers, C. R., & Sethna, J. P. (2007). Universally sloppy parameter sensitivities in systems biology models. *PLoS computational biology, 3*(10), e189.